Mapping Cerebral Connectivity Changes after Mild Traumatic Brain Injury in Older Adults Using Diffusion Tensor Imaging and Riemannian Matching of Elastic Curves

Andrei Irimia[1], *Di Fan*[1], *Nikhil N. Chaudhari*[1], *Van Ngo*[1], *Fan Zhang*[2], *Shantanu H. Joshi*[3], *Lauren J. O'Donnell*[2]

[1]Leonard Davis School of Gerontology, University of Southern California, Los Angeles CA USA
[2]Laboratory of Mathematics in Imaging, Harvard Medical School, Boston, MA USA
[3]Department of Neurology, Geffen School of Medicine, University of California, Los Angeles, CA USA

ABSTRACT

Although diffusion tensor imaging (DTI) can identify white matter (WM) alterations due to mild cases of traumatic brain injury (mTBI), the task of within-subject longitudinal matching of DTI streamlines remains challenging in this condition. Here we combine (A) automatic, atlas-informed labeling of WM streamline clusters with (B) streamline prototyping and (C) Riemannian matching of elastic curves to quantitate within-subject WM changes, focusing on the arcuate fasciculus. The approach is demonstrated in a group of geriatric mTBI patients imaged acutely and ~6 months post-injury. Results highlight the utility of differential geometry approaches when quantifying brain connectivity alterations due to mTBI.

Index Terms— Traumatic brain injury, diffusion tensor imaging, Riemannian matching, elastic curve

1. INTRODUCTION

Mild traumatic brain injury (mTBI) impacts over 1.7 million Americans every year, and its all-time prevalence in US adults has been estimated to exceed 10% [1]. Whereas the magnetic resonance imaging (MRI) of moderate-to-severe TBI is frequently positive for intraparenchymal hemorrhage and mass edema, the MRI readings of mTBI patients are often free of such findings despite victims' persistent neurocognitive deficits as late as one year after injury. mTBI frequently results in traumatic axonal injury (TAI) despite the absence of gross pathology on T_1- and T_2-weighted MRI, such that there has been increasing interest in mapping the effects of mTBI upon the white matter (WM) connectivity of the brain over time [1].

MRI studies of mTBI have frequently leveraged diffusion MRI (dMRI) to quantify the fractional anisotropy (FA) of water in the brain and to indicate that relatively-low FA may be indicative of TAI [2]. Although some research has focused on identifying (sub-) acute mTBI effects upon WM, few investigations have studied such phenomena longitudinally. One key reason for this is the scarcity of dependable techniques for longitudinal evaluation of WM connectivity using dMRI. Tract-based spatial statistics (TBSS) is a well-known approach for comparison within and across subjects, and this technique is available within the FMRIB Software Library (FSL) software library. Although appropriate for voxel-by-voxel analysis of WM properties, TBSS is inadequate for the quantification of FA alterations along WM streamlines. By contrast, a method called tract-based morphometry (TBM) utilizes a detailed dMRI-based WM atlas to enable the identification of WM fasciculi across and within subjects, in addition to their categorization into WM bundle clusters [4]. If used together with streamline prototyping [5], this approach allows the identification of WM connections fiducially to quantify changes in FA.

When comparing WM streamline properties longitudinally using dMRI, one important operation involves the matching of WM streamlines across time points. In this contribution, we propose that this task can be addressed using a novel combination of three sequential procedures, i.e. (A) automatic, atlas-informed labeling of WM streamline clusters, (B) streamline prototyping, and (C) modeling streamline prototypes as elastic curves which undergo Riemannian matching to calculate point-to-point correspondence. In this last step, points along (A) a streamline whose trajectory is inferred from dMRI data acquired at an initial (acute) timepoint are matched to corresponding points along (B) the streamline's trajectory as imaged at a second (chronic) timepoint. The approach is demonstrated in a group of geriatric mTBI victims imaged both acutely (within two weeks after injury) and chronically (about 6 months after injury). Our results highlight the utility of scale-invariant elastic curve matching for the quantification of WM alterations associated with mTBI in a geriatric patient population.

2. METHODS

2.1. Participants

The study received approval from the Institutional Review Board of the University of Southern California. All participants gave written informed consent. Participants had suffered an mTBI ~6 months (mo) before data acquisition (μ = 5.6 mo, σ = 0.2 mo) and had had acute Glasgow Coma Scale (GCS) scores over 12. They were older adults (N = 21; 8 females; age: μ = 66.2 y, σ = 7.8 y, range: 50-79 y) with no history of psychiatric or neurological prior to mTBI.

2.2. MRI acquisition

Anatomic T_1-, T_2-MRI and dMRI volumes were acquired at 3 T (Prisma MAGNETOM Trio TIM, Siemens Corp., Erlangen, Germany). T_1-weighted images were obtained by means of a 3D magnetization-prepared rapid acquisition gradient echo (MP-RAGE) sequence [parameters: repetition time (T_R) = 1.95 s; echo time (T_E) = 2.98 ms; inversion time (T_I) = 900 ms; voxel size = 1.0 × 1.0 × 1.0 mm]. T_2-weighted images were obtained using a 3D sequence (T_R = 2.5 s; T_E = 360 ms; voxel size = 1.0 × 1.0 × 1.0 mm). Diffusion MRI volumes were obtained in the axial plane and in 64 gradient directions (T_R = 8.3 s; T_E = 72 ms; voxel size = 2.7 × 2.7 × 2 mm). A volume with b = 0 s/mm^2 and one with b = 1,000 s/mm^2 were also obtained. All data were de-identified after their acquisition.

2.3. Preprocessing

Motion and eddy current artefact corrections were implemented using the FSL toolbox (fsl.fmrib.ox.ac.uk/fsl). Extra-cerebral voxels were excluded from analysis using the FSL brain extraction tool (BET). Diffusion tensor estimation, dMRI two-tensor tractography and FA computations were carried out in 3D Slicer (slicer.org). WM bundles shorter than 4 cm were discarded. This threshold was selected because the dMRI clustering algorithm is not optimal for processing relatively short streamlines whose length is below this empirically inferred threshold.

2.4. WM parcellation

An atlas for streamline clustering [3] was used to implement WM streamline parcellation. Briefly, the atlas facilitates WM connectivity parcellation into 800 clusters. An annotation method which leveraged population-based brain anatomical information and expert neuroanatomical knowledge was used to annotate and categorize streamline clusters. WM structure annotation was implemented in an atlas incorporating deep WM bundles—not excluding important long-range projection and association bundles— bundles related to cerebellar connections, commissural bundles and bundles connecting the brainstem, and both medium- and short -range superficial clusters categorized based on their inter-lobar connectivity. Potential type I errors were marked to enable their exclusion.

2.5. Streamline prototyping

Upon parcellation, each cluster's representative streamline was found using an approach for streamline prototyping [4-6]. Briefly, this strategy can be used for each cluster to enable the identification of a single WM streamline whose path, torsion and similar properties are typical of the cluster's streamlines. Prototyping is needed in part because dMRI tractography can generate artefactual streamlines which do not correspond to physical connections. Thus, the streamline cluster prototype is a more trustworthy descriptor of a cluster's true WM structure.

2.6. Streamline projection

Before quantifying WM changes across timepoints, the weighted average FA along the mean trajectory of each cluster's streamlines was computed as follows. First, a weighted mean FA was calculated based on information provided at each dMRI voxel within the spatial extent of the cluster. The weighting reflected the extent to which streamlines in the cluster shared the trajectory and length of the prototype. Second, the weighted mean FA values were assigned to points along the cluster's prototype streamline; this ensured that FA values along the prototype streamline were weighted averages of FA values along the trajectories of cluster streamlines. Thus, the streamline prototype fiber reflected not only the weighted average of cluster streamline trajectories, but also the weighted average of the FA along these streamlines. Because calculating the weighted average of streamline FA values along the prototype streamline can be conceptualized in terms of 'projecting' the FA values along individual streamlines upon the prototype streamline, we refer to this process as *streamline projection*.

2.6. Curve matching

After streamline projection, the curves associated with each cluster's streamline prototype—as resolved at each time point—were matched. This step was necessary because streamline prototypes' trajectories can vary subtly across time points even within the same subject. Thus, to obtain an accurate calculation of FA differences across time points, vertices along prototype trajectories must be matched across time points. To address this curve matching task, we model streamline prototypes as shapes using square root velocity functions (SRVFs), i.e. as elements in a space of curves with an infinity of dimensions [7-9]. The space is described by an appropriate Riemannian metric defined on the tangent space.

Shape matching between streamlines is enabled by calculating shortest length paths (i.e. geodesics) between shapes. The geodesic measures path length and quantifies the geometric distance between shapes; it also represents the best geometric deformation highlighting anatomical differences between them. Instead of computing maximum density paths of streamline bundles and computing geodesics between them *across* subjects, we compute instead geodesics *within* subjects but across time points. The mathematical details of Riemannian curve matching as related to our contribution are described elsewhere [7-9].

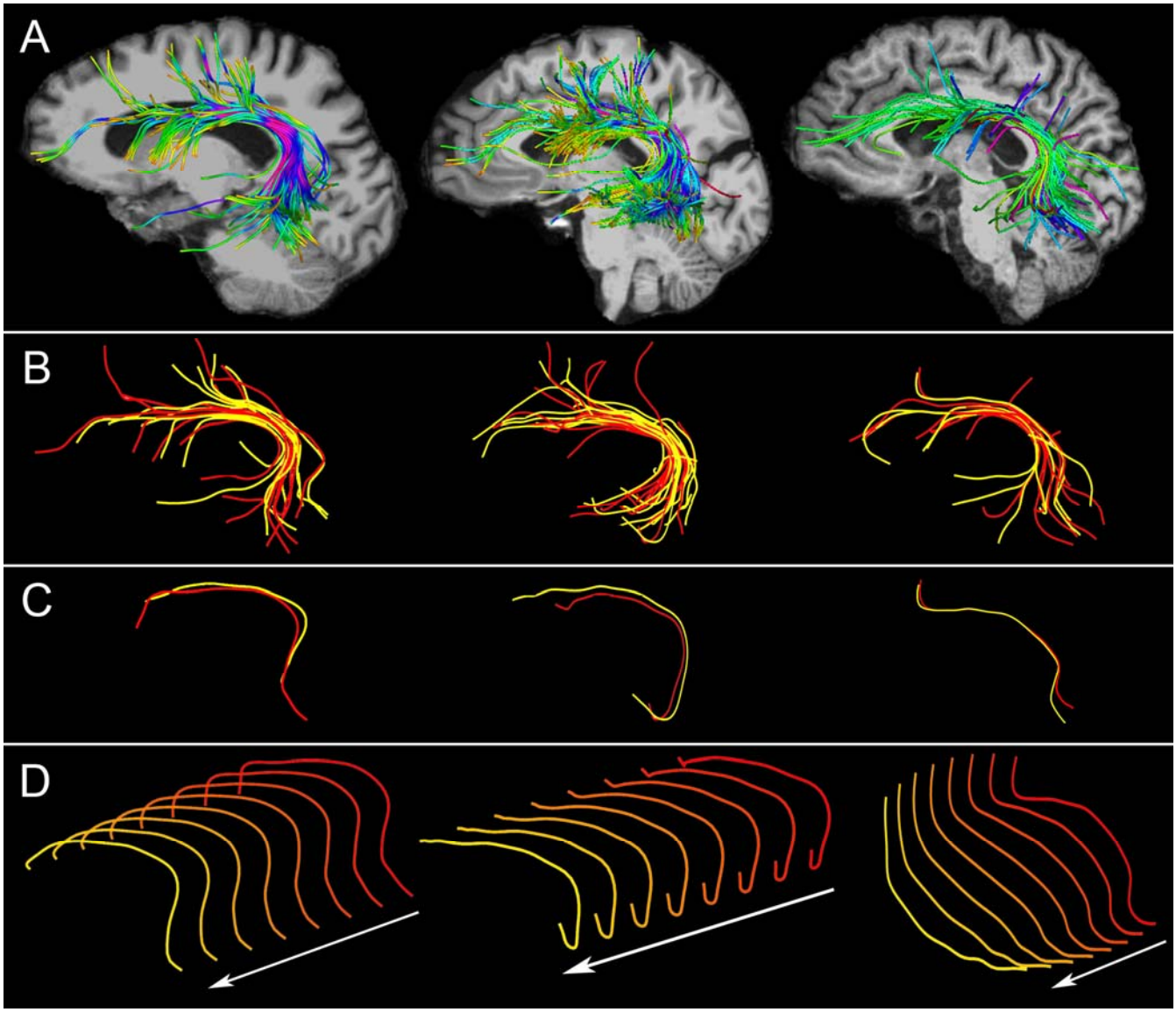

Figure 1. Longitudinal comparison and quantification of WM streamlines using DTI and Riemannian matching of elastic curves. Each column displays results from a different subject. (A). Automatically segmented streamlines of the arcuate fasciculus (AF) are superimposed to a skull-stripped, T_1-weighted sagittal slice of the brain. Color encodes streamline orientation at each location (red: left to right; green: anterior to posterior; blue: inferior to superior). (B) Streamline prototypes are calculated for AF clusters both at the acute time point (red, within two weeks post-injury) and at the chronic time point (yellow, ~6 months post-injury). (C) Separate depictions of sample pairs of prototype streamlines from each subject highlight inter-subject variability in prototype length and trajectory. (D) Riemannian matching of elastic curves facilitates the process of identifying a point-to-point correspondence between the prototype streamlines associated with the acute (red) and chronic (yellow) time points, respectively. Intermediate steps of the matching process are drawn using different colors from a palette ranging from red to yellow and indicating the transition from the first to the second time point (see arrow directions). Curves may not look identical when comparing (C) to (D) because the angle from which they are viewed in (D) is chosen to facilitate visualization of all intermediate steps of the curve matching process with minimum overlap.

3. RESULTS AND DISCUSSION

All 21 older adults included in the analysis had their WM fasciculi segmented, prototyped and matched across time points. Leveraging the methodological approach proposed here enabled the identification of time-related FA decreases ranging from ~1% to ~17% of their initial values. Across subjects, 13.2% ± 2.9% of all clusters had mean FA values which decreased by a mean of 11.8% ± 5.3% within the first six months after injury. FA decreases were identified throughout the WM, particularly in the inferior inferior longitudinal, fronto-occipital and superior longitudinal fasciculi. This is unsurprising because these relatively long WM bundles encompass much of the anteroposterior axis of the cortex. The bundles' relationship with FA changes may reflect coup-contrecoup effects due to fronto-occipital TBI, which is known to be relatively frequent [10]. Figure 1 provides a conceptual summary of the procedures utilized to implement (A) automatic WM segmentation, (B) streamline prototyping, (C) the alignment of individual prototype

streamlines, and (D) the calculation of a point-to-point correspondence using Riemannian matching of elastic curves. The figure shows results for three representative subjects: a 56-yo male, a 56-yo female, and a 70-yo male (first, second and third columns, respectively). The arcuate fasciculus (AF) is selected for illustration in (A) due to its characteristic shape, whose streamlines curve together in the vicinity of the temporo-parieto-occipital junction to connect Broca's and Wernicke's areas. In (B), the individual variability in AF trajectories across subjects is made apparent. Prototype streamlines are displayed in red for the acute time point and in yellow for the chronic time point. The number of prototypes is equal to the number of automatically segmented WM clusters assigned to the AF by the streamline labeling procedure. Visual inspection of (C) underscores the fact that, even within the same WM cluster, streamline prototype trajectories vary across time points; this highlights the need for implementing curve matching to calculate a point-to-point correspondence. (D) visually captures the curve matching process by displaying not only the two curves which are matched (red and yellow), but also intermediate steps of the matching process (see Figure). Because alternative strategies for longitudinal dMRI analysis are very different from our own, it is difficult to compare the present method to previous results in the literature. TBSS, for example, performs voxel-wise analysis but cannot make inferences pertaining to DTI-derived WM streamlines. Similarly, comparing the average FA of an entire structure (e.g. the AF) across time points may not be appropriate due to the potential effects of artefact variability across scans; it also may not be meaningful due to the substantial range of FA values within large WM structures. Nevertheless, further comparison of this method with prior methods should be undertaken in the future. Additionally, the method should be used to study healthy cohorts both in aging and development.

4. CONCLUSION

Because TBI is a highly heterogenous neurological condition, WM structures are differentially impacted by injury. Although mTBI patients' neurocognitive sequelae can be strikingly similar, hardly any patients experience identical injury patterns. Using a combination of (A) automatic, atlas-informed labeling of WM streamline clusters, (B) streamline prototyping and (C) Riemannian matching of elastic curves, we have quantified within-subject changes in WM structure properties and found substantial WM changes in a subset of WM bundles. Our results not only support the hypothesis that mTBI is associated with FA decreases, but also provide an illuminating demonstration of how our unique combination of quantitative approaches can be used to identify WM degradation after brain injury.

5. ACKNOWLEDGMENTS

This research was supported by NIH grants R01 NS 100973, MH 119222 to LJO, P41 EB 015902 to LJO, P41 EB 015989 to LJO and U01 CA 199459 to LJO, K25 AA 024192 to SHJ, by DoD contract W81-XWH-1810413 to AI and by the USC Undergraduate Research Associate Program (URAP) to AI. The authors thank volunteers for their participation. The opinions expressed in this article are the authors' own and do not reflect the view of the National Institutes of Health, the Department of Health and Human Services, the Department of Defense or the United States government. The authors state no conflicts of interest.

6. REFERENCES

[1] X. Wu, I. I. Kirov, O. Gonen, Y. Ge, R. I. Grossman, and Y. W. J. R. Lui, "MR imaging applications in mild traumatic brain injury: an imaging update," vol. 279, pp. 693-707, 2016.

[2] C. Eierud *et al.*, "Neuroimaging after mild traumatic brain injury: review and meta-analysis," vol. 4, pp. 283-294, 2014.

[3] F. Zhang *et al.*, "An anatomically curated fiber clustering white matter atlas for consistent white matter tract parcellation across the lifespan," *Neuroimage,* vol. 179, pp. 429-447, Oct 1 2018.

[4] K. A. Rostowsky, A. S. Maher, and A. Irimia, "Macroscale white matter alterations due to traumatic cerebral microhemorrhages are revealed by diffusion tensor imaging," *Frontiers in Neurology,* vol. 9, 2018.

[5] L. J. O'Donnell and C. F. Westin, "Automatic tractography segmentation using a high-dimensional white matter atlas," *IEEE Transactions on Medical Imaging,* vol. 26, pp. 1562-1575, 2007.

[6] L. J. O'Donnell, C. F. Westin, and A. J. Golby, "Tract-based morphometry for white matter group analysis," *Neuroimage,* vol. 45, pp. 832-44, 2009.

[7] S. H. Joshi, E. Klassen, A. Srivastava, and I. Jermyn, "A novel representation for Riemannian analysis of elastic curves in R^n,", *2007 IEEE Conference on Computer Vision and Pattern Recognition,* pp. 1643-+, 2007.

[8] A. Srivastava, E. Klassen, S. H. Joshi, and I. H. Jermyn, "Shape Analysis of Elastic Curves in Euclidean Spaces,", *IEEE Transactions on Pattern Analysis and Machine Intelligence,* vol. 33, pp. 1415-1428, 2011.

[9] G. Prasad *et al.*, "Automatic clustering and population analysis of white matter tracts using maximum density paths," *Neuroimage,* vol. 97, pp. 284-295, 2014.

[10] A. Irimia, J. D. Van Horn, and P. M. Vespa, "Cerebral microhemorrhages due to traumatic brain injury and their effects on the aging human brain," *Neurobiology of Aging,* vol. 66, pp. 158-164, 2018.